

## ARTICLES

## Determination of the ${}^6\text{Li} \rightarrow \alpha + d$ asymptotic $D$ - to $S$ -state ratio by a restricted phase shift analysis

E. A. George<sup>1,2,\*</sup> and L. D. Knutson<sup>1</sup><sup>1</sup>Department of Physics, University of Wisconsin, Madison, Wisconsin 53706<sup>2</sup>Department of Physics, University of Wisconsin-Whitewater, Whitewater, Wisconsin 53190

(Received 10 June 1998)

We describe a new method for determining the asymptotic normalization constants of the  ${}^6\text{Li} \rightarrow \alpha + d$  wave function. This method is based on a phase shift analysis of  ${}^6\text{Li} + {}^4\text{He}$  elastic scattering data, with high partial wave parameters obtained from Coulomb-wave Born approximation calculations for  $d$ -exchange scattering. Applying this analysis to  ${}^6\text{Li} + {}^4\text{He}$  elastic scattering at  $E_{\text{c.m.}} = 2.2$  MeV, we obtain a value for the asymptotic  $D$ - to  $S$ -state ratio of the  ${}^6\text{Li} \rightarrow \alpha + d$  wave function of  $-0.025 \pm 0.006 \pm 0.010$ . [S0556-2813(99)01802-6]

PACS number(s): 27.20.+n, 24.10.-i, 25.70.-z

### I. INTRODUCTION

There is considerable interest in experiments that can provide information about the internal structure of the  ${}^6\text{Li}$  nucleus. As recently as a few years ago, exact quantum-mechanical calculations of bound state properties were possible only for  $A = 3$ . However, in recent years there has been a significant amount of progress in extending these realistic calculations to higher values of  $A$  (see, for example, Refs. [1,2]). This progress has added new relevance to measurements of the internal structure of few-nucleon systems.

The importance of  $D$ -state components of light nuclei is well understood. In general the  $D$ -state terms arise from the tensor force, and consequently  $D$ -state observables allow us to test our understanding of this component of the  $NV$  potential (see Refs. [3,4]). In  ${}^6\text{Li}$ , the small, negative quadrupole moment indicates that the tensor force plays a role, but obtaining further information about the nature of the non-isotropic components of the bound state wave function has proven to be difficult. Experimentally, the most directly accessible quantity is the asymptotic  $D$ -state to  $S$ -state ratio of the  ${}^6\text{Li} \rightarrow \alpha + d$  component of the wave function. The determination of this  $D$ - to  $S$ -state ratio, which we designate as  $\eta$ , has been the subject of several previous experimental and theoretical studies. The results obtained to date will be summarized in Sec. II.

Our purpose in the present paper is to describe a new method for determining  $\eta$ . This method involves the analysis of polarization measurements for  ${}^6\text{Li} + {}^4\text{He}$  elastic scattering at low energies. In our analysis we make use of measurements from Ref. [5] at  $E_{\text{c.m.}} = 2.2$  MeV. It is believed [6] that in this low-energy region there are large contributions to the scattering amplitude from the exchange scattering process in which a deuteron is exchanged between the two  $\alpha$ -particle clusters. This gives rise to a strong back-angle peak in the differential cross section (see Fig. 1). Because the

exchange process plays an important role, it is reasonable to suppose that the measurements (especially at back angles) are sensitive to details of the  ${}^6\text{Li} \rightarrow \alpha + d$  wave function. The difficulty is to find a reliable method for extracting the desired information.

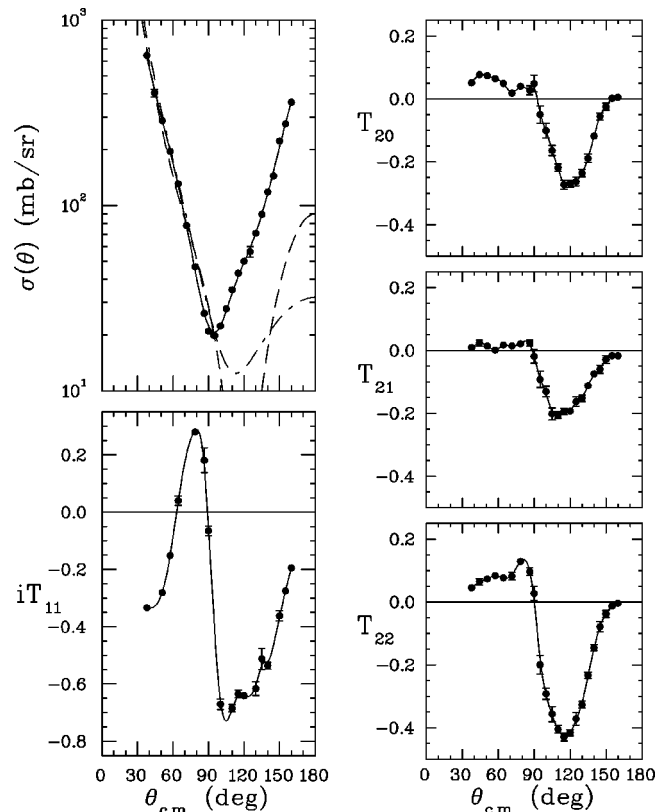


FIG. 1. Differential cross section and analyzing powers for  ${}^6\text{Li} + {}^4\text{He}$  elastic scattering at  $E_{\text{c.m.}} = 2.2$  MeV, from Ref. [5]. The error bars represent statistical errors only. Normalization errors are 4% for the differential cross section data, and about 10% for the analyzing power data. The solid line is a guide for the eye. The dashed (dash-dotted) line is the result of an optical model calculation using the set 1 (set 2) parameters in Table I.

\*Present address: Department of Physics, Wittenberg University, Springfield, Ohio 45501.

Processes that involve exchange graphs have frequently been analyzed in the past to obtain information about asymptotic wave functions. In few-nucleon systems this has most often been done by employing the ‘‘pole-extrapolation’’ method [7]. This method is based on the observation that for reactions involving exchange contributions, the analyzing powers at the location of the exchange pole depend in a simple way on the asymptotic wave function normalizations. The complication of this method is that for physical values of the incident particle energy, the exchange pole is located at an unphysical angle (i.e., an angle with  $z = \cos \theta < -1$ ). Therefore, what is normally done is to fit the measured observables in the physical region with some function, and then use that function to extrapolate the measurements to the pole, thereby allowing a determination of  $\eta$ . The treatment of systematic errors in the extrapolation is a difficult and controversial aspect of this method (see Refs. [8–10]). The proper treatment of Coulomb effects is also problematic. The effect of Coulomb repulsion between the projectile and the target is to change the pole into a cut, and there are further complications if (as in  ${}^6\text{Li} + {}^4\text{He}$  elastic scattering) the exchanged particle is also charged [11].

The new method we will describe here avoids these difficulties that are inherent in a pole-extrapolation analysis. The approach we use is to determine  $\eta$  by performing a restricted phase shift analysis of the  ${}^6\text{Li} + {}^4\text{He}$  elastic scattering data. The basic idea is as follows. For our kinematics, the exchange amplitude, when viewed as a function of energy and  $z = \cos \theta$ , has a cut that begins at  $z = -1.36$ . Since the branch point is close to the physical region, it is clear that an expansion of the amplitude in powers of  $\cos \theta$  will converge only slowly. This implies that in a partial-wave analysis the exchange scattering contribution converges slowly as a function of  $l$ . In contrast, one can show (see Sec. III C) that the direct scattering contributions converge rapidly. As a result, one finds a ‘‘window’’ in angular momentum space in which exchange scattering dominates by an order of magnitude or more over the remaining direct scattering contributions. Within this window the extracted phase shifts are small (typically only a few degrees). From this we infer that the scattering is ‘‘weak,’’ which means that the exchange scattering for these partial waves can be accurately calculated in Born approximation. The parameters of the bound-state wave function can thus be related to the elastic scattering measurements by carrying out a phase shift analysis that makes use of these calculated exchange scattering contributions in the higher partial waves. The method is described in more detail in Sec. III.

## II. PREVIOUS STUDIES OF ${}^6\text{Li}$ $D$ -STATE PARAMETERS

Several theoretical predictions for  $\eta$  have been obtained, based on various models of the  ${}^6\text{Li}$  wave function. Lehman and his collaborators [12,13] have used three-body ( $\alpha np$ ) models to obtain  $\eta \approx 0.01$ . Nishioka *et al.* [14] employed a simple  $\alpha + d$  cluster-model and found that wave functions with  $\eta \approx -0.014$  [3] reproduced the experimental value of the  ${}^6\text{Li}$  quadrupole moment. A recent shell-model calculation [15] predicts a quadrupole moment  $Q = -0.067 \text{ fm}^2$ , in good agreement with the currently accepted experimental value of  $-0.082$ , but unfortunately no results for  $\eta$  have

been reported for this calculation. Finally, a  ${}^6\text{Li}$  wave function with  $\eta = -0.07$  has been obtained by variational methods [16], although the quadrupole moment ( $Q = -0.8$ ) for this wave function is far too large in magnitude. A more recent calculation [2] gives a better result for the quadrupole moment [ $Q = -0.33(18) \text{ fm}^2$ ], but  $\eta$  is not reported. The authors of Ref. [2] point out that these variational method calculations are not very sensitive to the long-range properties of the wave function, and so the values obtained for  $Q$  and  $\eta$  are not yet expected to be reliable.

Only a few experimental studies of the  ${}^6\text{Li} \rightarrow \alpha + d$   $D$  state have been carried out. Bornand *et al.* [17] performed a forward dispersion relation analysis of  $d$ - $\alpha$  elastic scattering data and obtained values for the magnitudes of the  $S$ -state and  $D$ -state asymptotic normalization constants. The sign of  $\eta$  is not determined by this method, but the magnitude was found to be  $|\eta| = 0.005 \pm 0.014$ .

More recently, Santos *et al.* [18] compared tensor analyzing powers for  ${}^6\text{Li}(\vec{d}, \alpha)$  at 10 MeV with distorted-wave Born approximation (DWBA) calculations that included the effects of  $D$  states in both the  ${}^4\text{He} \rightarrow d + d$  and  ${}^6\text{Li} \rightarrow \alpha + d$  cluster wave functions. This group found that best fits to the data were obtained for  $-0.015 < \eta < -0.010$  when a  ${}^4\text{He}$  wave function with  $D$ -state parameter  $D_2 = -0.2$  was used.

Another determination of  $\eta$  was reported by Punjabi *et al.* [19], who measured tensor analyzing powers  $T_{20}$  at  $0.8^\circ$  for  ${}^1\text{H}({}^6\bar{\text{Li}}, d)$  at 4.5 GeV. The measurements were then compared with plane-wave impulse approximation calculations of  $T_{20}(q)$ , where  $q$  is the relative  $\alpha$ - $d$  momentum. A  ${}^6\text{Li}$  wave function with  $\eta \approx 0.02$  (obtained from a three-body model) predicts analyzing powers with the correct sign but slightly smaller in magnitude than the measured analyzing powers. These data thus favor a small but positive  $D$ -state to  $S$ -state ratio at small  $q$  values.

Finally, Green *et al.* [20] have compared  ${}^6\text{Li} + {}^4\text{He}$  elastic scattering data at  $E_{\text{c.m.}} = 11.1 \text{ MeV}$  to optical model plus  $d$ -exchange calculations, including transfers from  $2S$  and  $1D$  components of the ground-state  ${}^6\text{Li}$  wave function. They find that, in order for the calculations to not disagree with the measured tensor analyzing powers (in particular,  $T_{21}$ ), the  $D$ -state spectroscopic amplitude must lie in a range that, for their wave function, corresponds to  $0.00 > \eta > -0.08$ .

In summary, neither the experimental nor the theoretical determinations of  $\eta$  give unambiguous results. The two recent experiments at low energies seem to favor a negative value for  $\eta$ . However, it is not yet clear whether a negative  $\eta$  is theoretically compatible with the measured value of the quadrupole moment.

## III. EXCHANGE SCATTERING CONTRIBUTIONS TO PHASE SHIFT PARAMETERS

### A. Overview

We begin with a brief description of our method for determining  $\eta$  from  ${}^6\text{Li} + {}^4\text{He}$  elastic scattering data. The first step is to use the distorted-wave Born approximation (DWBA) (see Ref. [21]) to calculate  $d$ -exchange scattering contributions to the higher partial waves. In this calculation, a  ${}^6\text{Li} \rightarrow \alpha + d$  cluster wave function with both  $S$ - and  $D$ -state components is used at the reaction vertices. Coulomb waves

are used in the incoming and outgoing channels. The exchange amplitude calculated in this way is then used to obtain the  $S$  matrix (see Ref. [22]). From the  $S$  matrix, phase shifts and mixing parameters are extracted as outlined in Sec. III B. As discussed in Sec. III D below, the phase shift parameters obtained from this  $S$  matrix have a simple dependence on the asymptotic normalizations of the  $S$ - and  $D$ -state components of the wave function. This makes it possible to determine the asymptotic normalizations by carrying out a phase shift fit to  ${}^6\text{Li} + {}^4\text{He}$  elastic scattering data.

In the phase shift fit, the parameters describing the low partial waves are allowed to vary freely. The high partial wave parameters are taken from the calculation, with appropriate scale factors incorporated to allow for variation of the  $S$ - and  $D$ -state asymptotic normalizations. These scale factors are then varied along with the low- $l$  parameters to obtain the best fit to the data.

To demonstrate that this general approach is reasonable, we need to establish a few points. First, one must show that the contributions from the exchange scattering converge more slowly as a function of  $l$  than do the direct scattering contributions. This point is the subject of Sec. III C. It is also necessary to show that the phase shift parameters depend on the asymptotic parts of the  ${}^6\text{Li} \rightarrow \alpha + d$  wave function, and are insensitive to the interior details. This point is addressed in Sec. III D. The details of the exchange scattering calculation are given in the following section.

### B. Calculation of the exchange scattering partial-wave parameters

In this section we give a more detailed description of the method used to calculate the exchange scattering amplitude and the corresponding phase shift parameters. As noted earlier, we begin with the distorted-wave Born approximation. In this approximation the exchange amplitude  $f$  is given by

$$f = -\frac{\mu_\beta}{2\pi\hbar^2} \int \phi_{\text{Li}}^*(\mathbf{r}') \chi_C^{(-)*}(\mathbf{k}_f, \mathbf{r}') V \phi_{\text{Li}}(\mathbf{r}) \chi_C^{(+)}(\mathbf{k}_i, \mathbf{r}_\alpha) d\tau. \quad (1)$$

In this expression  $\phi_{\text{Li}}$  is the  ${}^6\text{Li}$  cluster bound-state wave

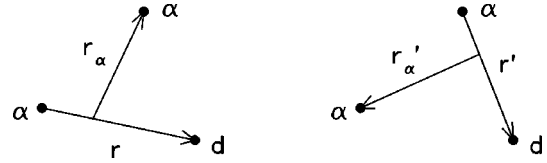


FIG. 2. Definition of the coordinates used in the distorted-wave Born approximation calculation for the initial (left) and final (right) states.

function,  $\chi_C^{(+)}$  and  $\chi_C^{(-)}$  are the  ${}^6\text{Li} + {}^4\text{He}$  scattering wave functions with, respectively, ingoing and outgoing spherical wave boundary conditions, and  $V$  is the transition potential. The coordinates for the initial and final states are defined in Fig. 2. For the scattering wave functions we use a purely Coulomb interaction corresponding to a uniformly charged sphere of radius 4.4 fm. The transition potential  $V$  includes a full three-body Coulomb term at each vertex. Since the calculations employ Coulomb distorted waves we refer to them as CWBA calculations.

The calculations were performed using a locally modified version of the full finite-range DWBA code PTOLEMY [23]. To test the numerical calculations, we performed an analytic calculation of the exchange amplitude in plane-wave Born approximation (PWBA), and compared the resulting  $S$ -matrix elements with the results of PTOLEMY calculations in which the Coulomb potentials were set to zero. With the appropriate sign conventions for the PTOLEMY matrix elements, there is good agreement between the analytic results and the PTOLEMY results.

After obtaining the  $S$ -matrix elements in the CWBA from PTOLEMY, we extracted the phase shifts and mixing parameters. For mixed angular momentum states, we used the Blatt-Biedenharn parametrization [24] in the Born approximation limit (that is, for small phase shifts and mixing parameters). The relation between the  $S$ -matrix elements and the phase shifts and mixing parameters is, for unmixed angular momentum states

$$S = e^{2i\delta} \approx 1 + 2i\delta \quad (2)$$

and for mixed states

$$S = \begin{pmatrix} \cos^2 \epsilon e^{2i\delta_1} + \sin^2 \epsilon e^{2i\delta_2} & \frac{1}{2} \sin 2\epsilon (e^{2i\delta_1} - e^{2i\delta_2}) \\ \frac{1}{2} \sin 2\epsilon (e^{2i\delta_1} - e^{2i\delta_2}) & \cos^2 \epsilon e^{2i\delta_2} + \sin^2 \epsilon e^{2i\delta_1} \end{pmatrix} \approx \begin{pmatrix} 1 + 2i\delta_1 & 2i\epsilon(\delta_1 - \delta_2) \\ 2i\epsilon(\delta_1 - \delta_2) & 1 + 2i\delta_2 \end{pmatrix}. \quad (3)$$

Here  $S$  is the  $S$ -matrix element obtained from the PTOLEMY calculation, the  $\delta$ 's are the phase shifts, and  $\epsilon \equiv \epsilon(j^\pi)$  is the mixing parameter that connects two states having the same total angular momentum  $j$  and parity  $\pi$ . Given the  $S$ -matrix elements, it is then straightforward to obtain the phase shifts and mixing parameters which are needed for the phase shift analysis.

### C. Comparison of direct and exchange scattering contributions

As we have mentioned earlier, our method for determining  $\eta$  relies on the assumption that the direct scattering contributions converge rapidly as a function of  $l$ , so that a window exists in angular momentum space in which the exchange scattering contributions dominate. Using the

TABLE I. Optical model potential parameters for the calculations shown in Fig. 1. Set 1 is the tenth set in Table 1 of Ref. [25]; set 2 is the sixteenth set in the same table. A Coulomb potential with  $R = 3.49$  fm and  $R = 3.60$  fm, respectively, was also included.

Optical model parameters:			
	$V$ (MeV)	$R$ (fm)	$a$ (fm)
Set 1			
real central	188.7	3.49	0.64
volume imaginary	9.4	3.49	0.64
Set 2			
real central	150.7	3.60	0.43
volume imaginary	11.2	3.60	0.43

method outlined in the preceding section we can now easily determine the exchange scattering as a function of  $l$ . It is also fairly straightforward to make reasonable estimates of the convergence rate of the direct scattering.

In a semiclassical picture one expects the direct scattering to be significant up to a maximum relative orbital angular momentum  $l_{\text{max}} < kR$ , where  $k$  is the wave number for the relative motion, and  $R \approx R_1 + R_2$ . For  ${}^6\text{Li}$  on  ${}^4\text{He}$  at  $E_{\text{c.m.}} = 2.2$  MeV, with  $R_i = 1.5A_i^{1/3}$ , we obtain  $l_{\text{max}} \approx 3$ . This suggests that the direct scattering contributions should be small beyond  $l = 3$ .

This result can be tested more rigorously by using an optical model to estimate the direct scattering. The optical model calculations were carried out with a code that makes use of subroutines borrowed from PTOLEMY. Calculations were performed with nine different  ${}^6\text{Li} + {}^4\text{He}$  potentials obtained from Refs. [20,25]. In Fig. 1, we show the results of calculations of the differential cross section, corresponding to two representative optical model potentials (the tenth and sixteenth parameter sets listed in Table 1 of Ref. [25]). The Woods-Saxon parameters for these two potentials are given in Table I. The first of the two potentials gives the largest phase shift parameters at high  $l$  of the nine potentials tested. The second potential produces what we judged to be the best overall fit to the data. Note that both potentials produce a back-angle peak in the cross section, but this peak is at least an order of magnitude smaller than the data. Because this failure to reproduce the size of the back-angle peak is a general feature of the optical model potentials we examined at this energy, we take this as evidence that exchange scattering is important.

In Table II, we list the phase shifts obtained from the

TABLE II. Comparison of average phase shifts (in degrees) extracted from the optical model calculations of Table I, and from CWBA calculations of the exchange amplitude.

phase shifts	set 1	set 2	CWBA
${}^3S$	-33.2	-22.8	137.9
${}^3P$	38.5	-22.9	-63.0
${}^3D$	-0.62	0.56	24.4
${}^3F$	0.64	-0.49	-9.0
${}^3G$	0.42	-0.09	3.3
${}^3H$	0.09	0.004	-1.3

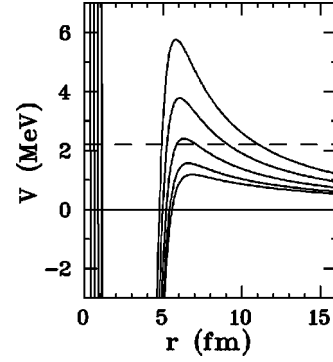


FIG. 3. Radial dependence of the real part of the set 2 (Table I) potential plus the centrifugal potential for  ${}^6\text{Li} + {}^4\text{He}$  elastic scattering at  $E_{\text{c.m.}} = 2.2$  MeV, plotted for angular momenta  $l = 0$  through  $l = 4$ .

S-matrix elements for both of these optical model potential parameter sets. The phase-shift parameters obtained from the optical model are found to be substantial for  $l \leq 3$ , but above  $l \approx 3$ , these parameters fall off quickly. By  $l = 5$ , the phase shift parameters derived from the optical model calculations are all 0.09 degrees or less. Also shown in Table II are the phase shift parameters obtained from the exchange scattering calculations described in Sec. III B. For ease of comparison the phase shifts for each  $l$  have been averaged over  $j$ . We see that the CWBA phase shifts fall off by a factor of 2–3 per  $l$  value rather than the typical order of magnitude per  $l$  value at large  $l$  for the optical model phase shifts. At  $l = 3$  the exchange scattering phases are roughly an order of magnitude larger than the corresponding direct scattering phase shifts obtained from the optical model.

From the values in the table, it is also apparent that for  $l \geq 3$ , where the exchange scattering dominates over the direct scattering, the exchange scattering phase shift parameters are small in magnitude. This supports the assumption that the exchange scattering contributions for the high  $l$  values can be accurately calculated in the Born approximation.

#### D. Sensitivity to asymptotic normalization constants

Next, we address the question of whether the method we have outlined is capable of providing reliable information about the asymptotic parts of the wave function. In particular, we wish to demonstrate that the exchange scattering amplitudes for large  $l$  are insensitive to the details of the interior of the bound state  ${}^6\text{Li}$  wave function.

There are good reasons to expect that this might be the case. Since our analysis is being carried out at low energy and since we are concerned only about large  $l$ , it can be argued that the reactions take place peripherally. In Fig. 3 we show the radial dependence of the effective potential (Coulomb plus centrifugal plus nuclear) for  $l = 0$  through  $l = 4$ . The nuclear potential used to generate these curves was the set 2 optical model potential of Table I. The point here is that for high  $l$  the Coulomb plus angular momentum barrier keeps the target and projectile well separated. For example, for  $l = 4$  the minimum separation is about 10 fm if we neglect tunneling (the barrier penetration probability [26] in this case is about 0.04).

To investigate this idea more thoroughly we have carried out a series of CWBA calculations employing a variety of different  ${}^6\text{Li}$  wave functions. In order to interpret these calculations we must first understand how the phase shifts and mixing parameters are expected to scale.

To begin, we note from Eq. (1) that the exchange amplitude involves two factors of  $\phi_{\text{Li}}$ . Therefore the  $S$ -matrix elements contain terms that are quadratic in the  $S$ -state wave function, terms that are quadratic in the  $D$  state, and  $SD$  cross terms. As a result, if one were to simply vary the overall normalizations of the  $S$ - and  $D$ -state parts of the wave function, the calculated  $S$ -matrix elements would scale according to

$$S = N_S^2 S_{SS} + N_S N_D S_{SD} + N_D^2 S_{DD}. \quad (4)$$

In our analysis the contributions from the  $DD$  term are always less than 1% and therefore these contributions are neglected. We may then disentangle the  $SS$  and  $SD$  contributions by carrying out separate CWBA calculations with and without the  $D$ -state term present in  $\phi_{\text{Li}}$ .

It is clear, therefore, that if the calculations are sensitive only to the asymptotic portions of the wave function (and not to the interior details), the calculated  $S$ -matrix elements should scale with the asymptotic normalization constants  $C_0$  and  $C_2$  according to the rule

$$S = C_0^2 S_{SS} + C_0 C_2 S_{SD}, \quad (5)$$

where we have dropped the  $DD$  term.

From Eq. (3) we can now show how the phase shifts and mixing parameters should scale. In the  $S$ -state-only calculation there is no spin dependence and so the  $S$  matrix is diagonal. In addition, one finds that diagonal elements for given  $l$  are independent of  $j$ . Therefore, neglecting the  $DD$  contributions we find that individual phase shifts should scale as  $\delta = C_0^2 \delta_{SS} + C_0 C_2 \delta_{SD}$  and that the splitting between two phase shifts of the same  $l$  and different  $j$  should scale as  $C_0 C_2$ . For the mixing parameters we note that the leading contribution to the off-diagonal  $S$ -matrix element will be proportional to  $C_0 C_2$ , and therefore the mixing parameters should scale approximately as  $C_2/C_0$ .

In order to investigate whether these scaling laws hold, we carried out a series of CWBA calculations. In these calculations we employed seven different  ${}^6\text{Li}$  wave functions. All of the wave functions were generated using the separation-energy procedure. For both  $S$  and  $D$  states, a real central potential of Woods-Saxon type was used, together with a Coulomb potential. The Woods-Saxon potential depth was adjusted to reproduce the experimental value of the separation energy for the cluster, 1.47 MeV.

The primary wave function used throughout our analysis is one generated with the parameters of Ref. [27], that is, with a real central potential with radius  $R = 1.9$  fm, diffuseness parameter  $a = 0.65$  fm, and Coulomb radius parameter  $r_C = 1.5$  fm. The  $S$ -state wave function has one node and a spectroscopic amplitude of 1.12. The  $D$ -state wave function also has a single node, and has a spectroscopic amplitude of  $-0.12$ . These spectroscopic amplitudes were chosen based on preliminary fits to the data. The asymptotic normalization constants are  $C_0 = 2.91$  and  $C_2 = -0.0684$ , corresponding to

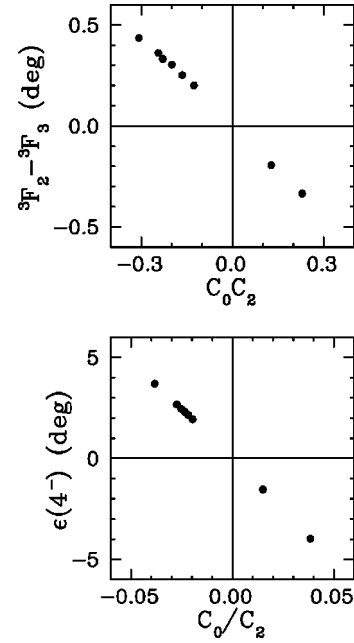


FIG. 4. Phase shift parameters calculated for exchange scattering in the CWBA with seven different  ${}^6\text{Li}$  wave functions, showing dependence on asymptotic normalization constants of the wave function ( $C_0$  and  $C_2$ ). The top graph shows the  $F_2 - F_3$  splitting, and the bottom graph shows the  $\epsilon(4^-)$  mixing parameter.

$\eta = -0.0235$ . Although it is not entirely clear that the  $D$ -state wave function should have a node, we choose to include one since the calculations of Refs. [12,13,16] obtain a node in the  $D$  state when an  $n$ - $p$  tensor potential is included.

Four additional wave functions were generated by starting with the same basic potential and changing the well parameters one at a time, with the remaining parameters fixed at the original values. Wave functions with  $R = 1.5$  fm,  $R = 2.3$  fm,  $a = 0.5$  fm, and  $a = 0.8$  fm were used. The sixth wave function was generated with the same radius and diffuseness parameters as the basic wave function, but without the node in the  $D$  state. The seventh wave function (from Ref. [20]) had  $R = 2.33$  fm,  $a = 0.71$  fm,  $r_C = 1.3$  fm, and no nodes in the  $D$  state, with spectroscopic amplitudes of 0.83 for the  $S$  state and 0.20 for the  $D$  state.

These seven wave functions were used to explore the dependence of the calculated phase shifts and mixing parameters on the asymptotic normalization constants. We find that the PTOLEMY phase shift parameters (for high  $l$  values) follow the expected scaling behavior to a very good approximation. Some representative examples are shown in Fig. 4. Here we see that splitting of the  ${}^3F_2$  and  ${}^3F_3$  phase shift parameters does, in fact, scale as  $C_0 C_2$ , and that the  $j = 4$  mixing parameter scales as  $C_2/C_0 = \eta$ .

This demonstration that the phase shift parameters scale in a simple way with the asymptotic normalization constants is important. What this means is that the phase shift fitting requires only a single CWBA calculation. For the high  $l$  values we take the phase shifts and mixing parameters from the calculation, and incorporate appropriate renormalization parameters which are then adjusted to fit the data. The renormalization parameters together with the asymptotic norms of the wave function employed in the CWBA calculation are

then combined to obtain the best fit asymptotic normalization parameters.

#### IV. THE PHASE SHIFT ANALYSIS

The  ${}^6\text{Li} + {}^4\text{He}$  elastic scattering angular distributions used in the phase shift analysis were obtained at the University of Wisconsin tandem accelerator laboratory. Angular distributions for the differential cross section, the vector analyzing power  $iT_{11}$ , and the tensor analyzing powers  $T_{20}$ ,  $T_{21}$ , and  $T_{22}$  were obtained at a  ${}^6\text{Li}$  incident energy of 5.5 MeV. The data, shown in Fig. 1, have typical normalization errors of 4% (cross section) and about 10% (analyzing powers). The experiment is described in more detail in Ref. [5].

The phase shift analysis of the data was performed with a code that uses the CERN library routine MINUIT [28] to perform the least-squares minimization. We carried out a large number of fits before reaching our final conclusions. In any given fit the various parameters (phase shifts, inelastic parameters, mixing parameters) were divided into two groups. The parameters in the low- $l$  group were treated as purely phenomenological quantities which are freely adjusted in the fit. The parameters in the high- $l$  group were calculated from the exchange amplitudes with adjustable  $S$ - and  $D$ -state multiplicative factors. In all of our fits, the the  $S$ -,  $P$ -, and  $D$ -wave phase shifts and inelastic parameters and the mixing parameters for  $j=1$  through  $j=4$  were included in the low- $l$  group.

One of the important steps in the analysis is to decide which parameters should be included in the high- $l$  group. These parameters eventually determine the asymptotic normalizations, and therefore one is assured of obtaining reliable results only if the corresponding partial waves are indeed dominated by exchange scattering. One of the main criteria we use in making this decision is consistency. It is possible to generate many different phase shift fits (for example, by moving parameters between the high- $l$  and low- $l$  groups or by floating or not floating the overall normalizations of the data) and if the analysis is reasonable one should obtain consistent results for the asymptotic normalizations as the details of the fit are varied. If a particular phase shift parameter seems to require asymptotic normalizations which are consistently well away from the values preferred for the majority of the parameters, one concludes that this parameter is affected by nonexchange contributions.

In our initial attempts to fit the data set we found that large splittings were required for all partial waves up through and including  $l=3$ . We were particularly concerned about the  $F$ -wave splittings since these seemed larger than one could explain either by exchange scattering (which should produce only small splittings) or by direct scattering (which was expected to be small for  $l=3$ ). It is now clear that the large  $F$ -wave splitting is caused by a  $4^-$  state at  $E_x = 6.56$  MeV in the  ${}^{10}\text{B}$  compound nucleus which is close to the energy at which the measurements were obtained ( $E_x = 6.66$  MeV). To verify that this is the correct interpretation we carried out a separate phase shift fit of the data shown in Fig. 1 together with  ${}^6\text{Li}(\alpha, \alpha){}^6\text{Li}$  excitation functions [29] at six angles covering  ${}^{10}\text{B}$  excitation energies from 6.44 to 6.68 MeV. We found that the analyzing power measurements and the energy-dependent cross sections can be reproduced si-

multaneously if one includes the  $4^-$  state at  $E_x = 6.56$  MeV along with a  $1^-$  state at 6.87 MeV [30]. If one then subtracts the resonant contribution from the  ${}^3F_4$  phase shift, the remaining  $F$ -wave phases are reasonably consistent with the expectations for pure exchange scattering.

In carrying out the trial fits it was found that several different phase shift parameters are capable of providing useful information about the  $D$ -state normalization. For our ‘‘final’’ fit we included in the high- $l$  group all the mixing parameters for  $j \geq 5$ , the  ${}^3F_3 - {}^3F_2$  splitting, and all of the  $l \geq 4$  phase shifts. In principle, each mixing parameter and each phase shift splitting could provide a separate determination of the  $D$ -state multiplicative factor. However, because the uncertainties in these parameters are correlated, we used a single common  $D$ -state multiplier for all parameters sensitive to this quantity.

The decision to include the  ${}^3F_3 - {}^3F_2$  splitting as one of the parameters that determines the asymptotic normalizations requires some justification. We note, first of all, that there are no nearby  $2^-$  or  $3^-$  states in the  ${}^{10}\text{B}$  compound nucleus, so these partial waves should be unaffected by resonance contributions. Second, we find that the  $D$ -state normalization determined from this parameter alone is consistent with the value obtained from the remaining parameters. With this in mind, we believe that the decision to include the  ${}^3F_3 - {}^3F_2$  splitting is justified, with the understanding that the final systematic error should reflect the uncertainties associated with possible nonexchange contributions. The assumption that the  $l=3$  partial waves are dominated by exchange scattering is certainly consistent with the results given in Table II.

#### V. RESULTS

Our final fit to the angular distribution data was obtained with the parameters shown in Table III. This set has 26 free parameters, and provides a fit to the data with a  $\chi^2$  per degree of freedom of 1.27, corresponding to a confidence level of 4% (see Fig. 5). The phase shifts for  $4 \leq l \leq 8$ , the mixing parameters for  $5 \leq j \leq 9$ , and the  ${}^3F_3 - {}^3F_2$  splitting were all determined from the exchange calculations, and scaled using the  $S$ - and  $D$ -state multiplicative factors. The overall normalizations of the individual cross section and analyzing power measurements were treated as free parameters in this final fit, but the results obtained for these quantities are consistent with the normalization errors quoted in Ref. [5].

Scaling the  $S$ - and  $D$ -state amplitudes of our original  ${}^6\text{Li}$  wave function by the renormalization parameters of our final fit gives the result  $C_0 = 2.91 \pm 0.09$  and  $C_2 = -0.077 \pm 0.018$ . This yields  $\eta = -0.026 \pm 0.006$ , where the error is purely statistical. Note that the value for  $C_0$  is in good agreement with that obtained by Blokhintsev *et al.* [31] from an energy-dependent  ${}^4\text{He} + d$  phase shift analysis,  $C_0 = 2.93 \pm 0.15$ .

The statistical uncertainty for each fitting parameter was determined in the usual way, as the square root of the corresponding diagonal element of the error matrix. For a given parameter, this is equivalent to the change in that parameter that would increase the overall  $\chi^2$  by 1, where the remaining parameters are varied to minimize  $\chi^2$ . This procedure was used to obtain the statistical errors for  $C_0$  and  $C_2$  quoted above.

TABLE III. Adjusted phase shift parameters for the fit shown in Fig. 5. The  $4 \leq l \leq 8$  phase shifts and the  $5 \leq j \leq 9$  mixing parameters were determined from the exchange scattering calculations, scaled by the appropriate  $S$ - and  $D$ -state multipliers. All phase shifts, mixing parameters and inelastic parameters are given in degrees.

	$j=l-1$	$j=l$	$j=l+1$
Phase shifts:			
$l=0$			-53.41
$l=1$	-29.23	-17.08	-19.30
$l=2$	64.64	33.71	4.95
$l=3$	-6.23 <sup>a</sup>	-4.94 <sup>a</sup>	-14.26
Inelastic parameters:			
$l=0$			0.00 <sup>b</sup>
$l=1$	7.10	8.69	8.97
$l=2$	0.41	0.00 <sup>b</sup>	0.99
$l=3$	1.03 <sup>c</sup>	1.03 <sup>c</sup>	1.03 <sup>c</sup>
Mixing parameters:			
$\epsilon(1^-)$	$\epsilon(2^+)$	$\epsilon(3^-)$	$\epsilon(4^+)$
16.04	4.63	19.94	-0.97
Normalizations:			
$\sigma(\theta)$	$iT_{11}$	$T_{20}$	$T_{21}$
1.02	1.08	1.01	1.02
$T_{22}$			
1.09			
S- and D-state multipliers:			
$N_S = 1.00 \pm 0.03$			
$N_D = 1.12 \pm 0.27$			

<sup>a</sup>The splitting of the  ${}^3F_2$  and  ${}^3F_3$  phases was determined from the  $S$ - and  $D$ -state multipliers.

<sup>b</sup>Inelastic parameters listed as 0.00 reach unphysical (negative) values in the fit and are therefore fixed at zero.

<sup>c</sup>The  $F$ -wave inelastic parameters were constrained to be equal.

The remaining problem is to estimate the systematic error. We do this by looking at the variation of the  $C_0$  and  $C_2$  values as we change the conditions of the fit. For example, a series of fits was carried out with different starting parameters. These fits produced at most a few percent change in the  $S$ - and  $D$ -state renormalization factors, and a change in the resulting value of  $\eta$  of no more than about  $\pm 0.001$ .

Next we performed several different fits with various inelastic parameters fixed or varying freely. For these fits, the value of  $\eta$  changed by no more than  $\pm 0.003$ .

We also looked at the effect of truncating the phase shift expansion at smaller values of  $l$ . Performing new phase shift fits with the  $L$ -,  $K$ -, and  $I$ -wave phase shift parameters and the  $j=6$  through  $j=9$  mixing parameters set successively equal to zero changed  $\eta$  by no more than  $\pm 0.004$ .

We then investigated the dependence of  $\eta$  on the choice of parameters to be included in the high- $l$  group. The parameters that seem to have the largest effect on  $\eta$  are the  ${}^3F_2$  -  ${}^3F_3$  splitting and the  $G$ - and  $H$ -wave phase shifts, with some additional significant contributions from the  $\epsilon(5^+)$  and  $\epsilon(6^-)$  mixing parameters. The role of each of these parameters was investigated by moving the parameters, one by one, from the high- $l$  group to the low- $l$  group and performing a new fit. In no case did the resulting value of  $\eta$  change by more than  $\pm 0.012$ , with the typical change being about  $\pm 0.008$ .

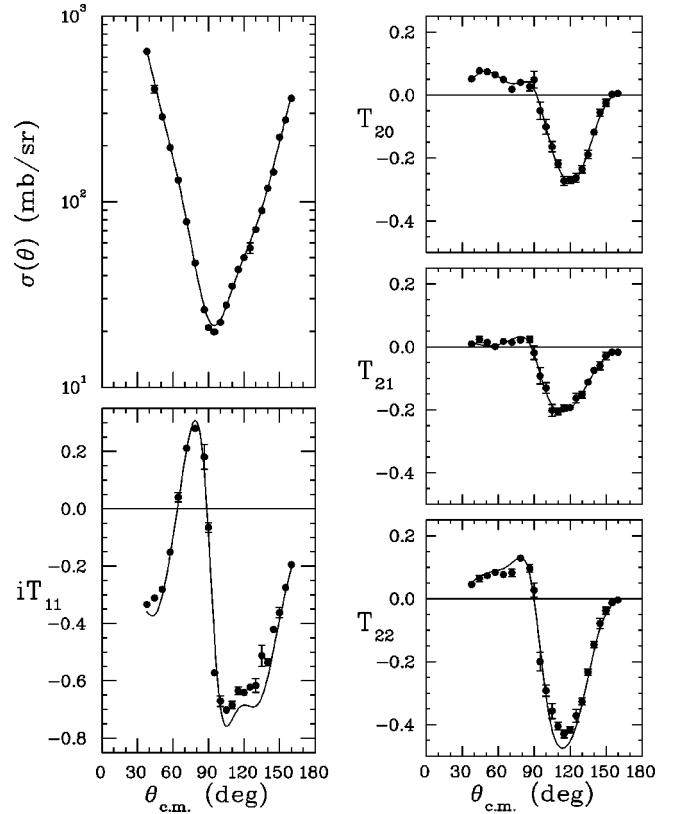


FIG. 5.  ${}^6\text{Li} + {}^4\text{He}$  elastic scattering data at  $E_{\text{c.m.}} = 2.2$  MeV, with the phase shift fit of Table III (solid line). The normalization of the data has not been adjusted.

Next, we explored possible systematic errors associated with the calculation of the high- $l$  phase shift parameters. First, we tested the sensitivity of our results to the nonasymptotic parts of the  ${}^6\text{Li} \rightarrow \alpha + d$  wave function that was used in the exchange calculation. For each of the six additional wave functions described in Sec. III D, we recalculated the  $d$ -exchange phase shifts and mixing parameters and used these in a new phase shift fit. In no case did the value of  $\eta$  determined from the fit change by more than  $\pm 0.001$ . In Fig. 6, the radial wave function used in the final fit reported in Table III, as well as the wave function that produced the greatest change in  $\eta$  (the wave function from Ref. [20]), are shown for comparison. Based on these results, the systematic error in  $\eta$  due to the choice of wave function is taken to be  $\pm 0.001$ .

In addition, we estimated the systematic error that arises from the assumption that contributions to the Coulomb distorted waves from nuclear potentials are negligible. We recalculated the exchange contributions to the phase shift parameters, using three different  ${}^6\text{Li} + {}^4\text{He}$  optical model scattering potentials in the incoming and outgoing scattering channels. The optical model potentials used were the tenth and sixteenth parameter sets from Table 1 of Ref. [25] and the second set from Table 2 of Ref. [20]. The first two parameter sets were the same ones used in the calculations shown in Fig. 1. The third set includes a spin-orbit potential. The resulting phase shift fits produced values of  $\eta$  that differ by no more than  $\pm 0.004$  from that obtained using high- $l$  phase shift parameters calculated in the CWBA. Taking all

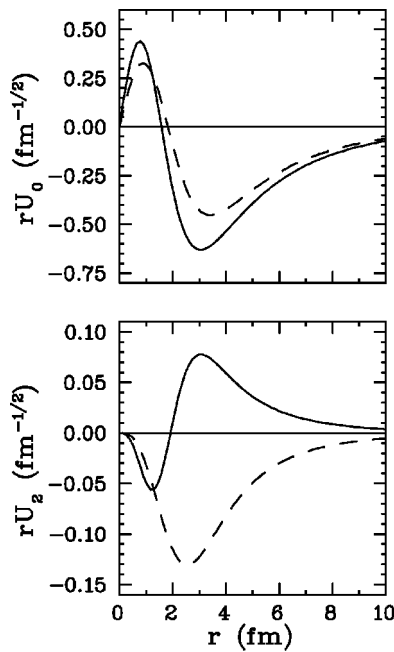


FIG. 6.  ${}^6\text{Li} \rightarrow \alpha + d$  radial wave functions. The solid line represents the wave function generated from a Woods-Saxon potential with  $R=1.9$  fm and  $a=0.65$  fm, as well as a Coulomb potential with radius parameter  $r_C=1.5$  fm [27]. The dashed line represents the wave function generated from a Woods-Saxon potential with  $R=2.33$  fm and  $a=0.71$  fm, and no node in the  $D$  state, as well as a Coulomb potential with radius parameter  $r_C=1.3$  fm [20].

of these effects into account, and assuming that the various systematic errors are uncorrelated, we estimate that the overall systematic error in  $\eta$  is approximately  $\pm 0.010$ .

## VI. SUMMARY

We have described a new method for determining the asymptotic normalization constants of the  ${}^6\text{Li} \rightarrow \alpha + d$  cluster wave function. This method is based on a phase shift analysis of elastic scattering data, with high partial wave parameters obtained from Coulomb-wave Born approximation calculations for  $d$ -exchange scattering. Applying this analysis to  ${}^6\text{Li} + {}^4\text{He}$  elastic scattering at  $E_{\text{c.m.}}=2.2$  MeV, we obtain a value for the asymptotic  $D$ - to  $S$ -state ratio of the  ${}^6\text{Li} \rightarrow \alpha + d$  wave function of  $-0.025 \pm 0.006 \pm 0.010$ . This value is consistent at the  $1\sigma$  level with the results obtained by Bornand *et al.* [17], by Green *et al.* [20], and by Santos *et al.* [18]. We believe that this method of determining the asymptotic  $D$ - to  $S$ -state ratio from low-energy elastic scattering data may be applicable to other systems as well.

Finally, we note that there are similarities between the method we describe here and a procedure that has been used to obtain values of the  $\pi NN$  coupling constants from  $NN$  elastic scattering data. In this latter procedure (see Ref. [32]), the Bonn peripheral model is used to predict heavy boson exchange contributions to high partial-wave phase shift parameters. Then, in order to reliably separate out the contributions of one-pion exchange, the coupling constants are obtained from fits based on only those parameters for which the theoretical one-pion exchange plus heavy boson exchange calculations are reasonably consistent with experiment.

## ACKNOWLEDGMENT

This work was supported in part by the National Science Foundation.

- 
- [1] B. S. Pudliner, V. R. Pandharipande, J. Carlson, and R. B. Wiringa, *Phys. Rev. Lett.* **74**, 4396 (1995).
  - [2] B. S. Pudliner, V. R. Pandharipande, J. Carlson, Steven C. Pieper, and R. B. Wiringa, *Phys. Rev. C* **56**, 1720 (1997).
  - [3] A. M. Eir3 and F. D. Santos, *J. Phys. G* **16**, 1139 (1990).
  - [4] D. R. Lehman, *J. Phys. (Paris)* **51**, 47 (1990).
  - [5] E. A. George, D. D. Pun Casavant, and L. D. Knutson, *Phys. Rev. C* **56**, 270 (1997).
  - [6] P. Tru3el and W. Bierter, *Phys. Lett.* **29B**, 21 (1969).
  - [7] R. D. Amado, M. P. Locher, and M. Simonius, *Phys. Rev. C* **17**, 403 (1978).
  - [8] B. Vuaridel, W. Gr3e3bler, V. K3nig, K. Elsener, P. A. Schmelzbach, M. Bittcher, D. Singy, I. Borb3ely, M. Bruno, F. Cannata, and M. D'Agostino, *Nucl. Phys.* **A499**, 429 (1989).
  - [9] J. T. Londergan, C. E. Price, and E. J. Stephenson, *Phys. Lett.* **120B**, 270 (1983).
  - [10] D. D. Pun Casavant, J. G. Sowinski, and L. D. Knutson, *Phys. Lett.* **154B**, 6 (1985).
  - [11] F. D. Santos, *Phys. Rev. C* **24**, 1379 (1981).
  - [12] D. R. Lehman and Mamta Rajan, *Phys. Rev. C* **25**, 2743 (1982).
  - [13] W. C. Parke and D. R. Lehman, *Phys. Rev. C* **29**, 2319 (1984).
  - [14] H. Nishioka, J. A. Tostevin, and R. C. Johnson, *Phys. Lett.* **124B**, 17 (1983); H. Nishioka, J. A. Tostevin, R. C. Johnson, and K.-I. Kubo, *Nucl. Phys.* **A415**, 230 (1984).
  - [15] D. C. Zheng, B. R. Barrett, J. P. Vary, W. C. Haxton, and C.-L. Song, *Phys. Rev. C* **52**, 2488 (1995).
  - [16] J. L. Forest, V. R. Pandharipande, Steven C. Pieper, R. B. Wiringa, R. Schiavilla, and A. Arriaga, *Phys. Rev. C* **54**, 646 (1996).
  - [17] M. P. Bornand, G. R. Plattner, R. D. Viollier, and K. Alder, *Nucl. Phys.* **A294**, 492 (1978).
  - [18] F. D. Santos, I. J. Thompson, and A. M. Eir3, *J. Phys. (Paris)* **51**, 443 (1990).
  - [19] V. Punjabi, C. F. Pedrisat, E. Cheung, J. Yonnet, M. Boivin, E. Tomasi-Gustafsson, R. Siebert, R. Frascaria, E. Warde, S. Belostotsky, O. Miklucho, V. Sulimov, R. Abegg, and D. R. Lehman, *Phys. Rev. C* **46**, 984 (1992).
  - [20] P. V. Green, K. W. Kemper, P. L. Kerr, K. Mohajeri, E. G. Myers, D. Robson, K. Rusek, and I. J. Thompson, *Phys. Rev. C* **53**, 2862 (1996).
  - [21] Norman Austern, *Direct Reaction Theories* (Wiley, New York, 1970).
  - [22] A. M. Lane and R. G. Thomas, *Rev. Mod. Phys.* **30**, 257 (1958).
  - [23] M. H. Macfarlane and S. C. Pieper, Report No. ANL-76-11 Rev. 1 (unpublished), modified by R. P. Goddard, 1980.
  - [24] J. M. Blatt and L. C. Biedenharn, *Rev. Mod. Phys.* **24**, 258 (1952).



- [25] H. G. Bingham, K. W. Kemper, and N. R. Fletcher, Nucl. Phys. **A175**, 374 (1971).
- [26] Leonard I. Schiff, *Quantum Mechanics* (McGraw-Hill, New York, 1968), p. 278.
- [27] K.-I. Kubo and M. Hirata, Nucl. Phys. **A187**, 186 (1972).
- [28] F. James, CERN Program Library Long Writeup D506 (unpublished), 1994.
- [29] V. Meyer, R. E. Pixley, and P. Truöl, Nucl. Phys. **101A**, 321 (1967).
- [30] F. Ajzenberg-Selove, Nucl. Phys. **A490**, 1 (1988).
- [31] L. D. Blokhintsev, V. I. Kukulín, A. A. Sakharuk, and D. A. Savin, Phys. Rev. C **48**, 2390 (1993).
- [32] D. V. Bugg and R. Machleidt, Phys. Rev. C **52**, 1203 (1995).